

****FULL TITLE****
*ASP Conference Series, Vol. **VOLUME**, **YEAR OF PUBLICATION***
****NAMES OF EDITORS****

2 types of spicules “observed” in 3D realistic models

Juan Martínez-Sykora

Institute of Theoretical Astrophysics, University of Oslo, Norway

Lockheed Martin Solar & Astrophysics Lab, Palo Alto, USA

Abstract.

Realistic numerical 3D models of the outer solar atmosphere show two different kind of spicule-like phenomena, as also observed on the solar limb. The numerical models are calculated using the *Oslo Staggered Code* (OSC) to solve the full MHD equations with non-grey and NLTE radiative transfer and thermal conduction along the magnetic field lines. The two types of spicules arise as a natural result of the dynamical evolution in the models. We discuss the different properties of these two types of spicules, their differences from observed spicules and what needs to be improved in the models.

1. Numerical Methods and description of the model

The nature of spicules observed at the solar limb have long been a mystery, in this paper we discuss two types of jets that occur naturally in 3D numerical models of the solar atmosphere. The MHD equations are solved in a model spanning the upper convection and corona using the *Oslo Stagger Code* (OSC). In addition, this code solves a rather realistic NLTE radiative transfer, including scattering, and thermal conduction along the field lines as explained in Martínez-Sykora et al. (2008).

The models described below have a grid size of $256 \times 128 \times 160$ points spanning $16 \times 8 \times 16$ Mm³. The grid is uniform in the horizontal direction with a grid spacing of 65 km. In the vertical direction the grid is non-uniform, ensuring that the vertical resolution is good enough to resolve the photosphere and transition region with a grid spacing of 32.5 km, while becoming larger at coronal heights. At these resolutions the models have been run for roughly 1.5 hours solar time. We have created two models with different average unsigned field in the photosphere; one with 16 G (A2) and the other 160 G (B1). In addition to this ambient field, we introduce a magnetic flux tube into the lower boundary at the bottom boundary (Martínez-Sykora et al. 2008).

2. Results and discussions

In the models we found two types of spicule-like structures, *i.e* the so-called type I (Martínez-Sykora et al. 2009) and type II (McIntosh et al. 2007).

A synthetic image of Ca II at the limb is shown in fig 1 which shows the two types of spicules. These structures look rather similar to what is observed at the limb in the Sun in Ca II.

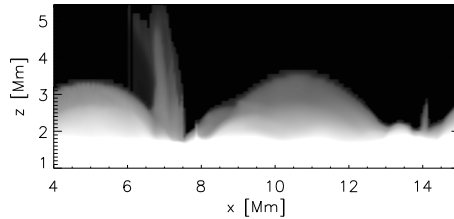


Figure 1. Synthetic image of Ca II H from the limb of the model. Observe the two types of spicules, type I located at $x = 14$ Mm and type II at $x = 7$ Mm. The synthetic image is done with MULTI3D.

Table 1 shows the differences between the two types of the spicules in our models and compared to observations. The reader is referred to work that has recently been completed related to spicules; Rouppe van der Voort et al. (2007); De Pontieu et al. (2007); Hansteen et al. (2006); Martínez-Sykora et al. (2009).

Type I	Type II	Observations
150 examples in both models	2 examples only in B1 model	Type II ubiquitous
Length $\approx [0.4, 1.5]$ Mm	Length ≈ 5 Mm	Type I are longer
Duration $\approx [2, 5]$ min	Duration ≈ 1 min	Type I have longer durations
Parabolic profile in time (deceleration)	Complex velocity profiles due to acceleration at different height	Seems to agree (see bibliography)
Up-downflow profile	Only upflow	Seems to agree
Velocities $\approx [5, 35]$ km/s	Velocities ≈ 150 km/s	Type I reach larger velocities
Observed in Ca II	Counterpart in Transition region emission lines	Seems to agree
Driven by magneto-acoustic shocks	Reconnection	Similar drivers suggested

Table 1. Properties of the two types of spicules “observed” in the models and compared with observations.

Most likely, the differences between the two types seem to agree with the observations. However, a deeper study needs to be done with the type II spicules found in the model (work in progress). Moreover, a closer comparison with the observations is required. It is interesting to note that the appearance of type I does not show a clear preference between models with or without flux emergence, while type II only appear in the model with the largest ambient ambient field (B1), and only after emerging flux cross the photosphere. Spicules of both types in the models are located at the footpoints of the atmospheric coronal loops, where the field lines are open field lines or at least penetrate into the corona. Moreover, the footpoint that is closer to the emerging flux tube is the one that shows most jets. The type II spicules shows a corresponding nearby hot loop

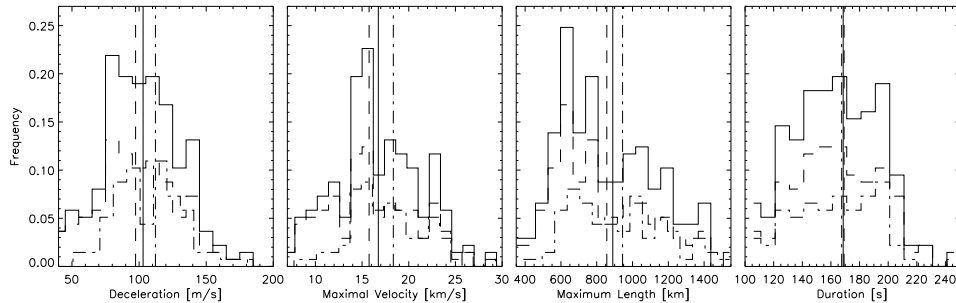


Figure 2. Histograms, normalized to the total number of spicules, for decelerations, maximal velocity, maximum lengths, and duration, from left to right, respectively, measured from the two models (B1 dash and A2 dash-dot line) and the sum (continuum line). The vertical line is the median value of the distribution. The two models show different distributions of the deceleration, maximum lengths, and duration, as well as some differences in maximum velocity. The model B1 shows on average slightly lower decelerations, shorter length, and shorter velocities than A2.

which also seems observed in the Sun (De Pontieu et al. 2009). The hot loop ($> 10^6$ K) can be observed with coronal emission lines.

In brief, we can summarize the differences between observations and models for type I spicules by noting that the upper limits of the deceleration, length, duration, and maximal velocity are smaller in the models (Martínez-Sykora et al. 2009). Histograms for deceleration, maximum length, maximal velocity and duration for the type I from the model are shown in fig 2. These can be compared with the histograms from the observations done by De Pontieu et al. (2007). They show an agreement in the lower part to the histograms, and the differences between the B1 and A2 seems similar to the differences of the two regions observed by De Pontieu et al. (2007). However, the models do not fit with the upper part of the observed histograms.

In order to improve the models we consider that the resolution of the box is important. The chromosphere is poorly resolved numerically and this affects the size of the structures of the spicules. In addition, low resolution might bring other effects like the diffusion of the shocks (type I) or of the magnetic discontinuity (type II). With higher resolution we expect sharper shocks, larger range of velocities, better resolved and more frequent spicules.

In models, it is also important to take time-dependent hydrogen ionization into account in the the upper chromosphere. The ionization of hydrogen in the solar chromosphere and transition region does not obey LTE, or instantaneous statistical equilibrium, as the timescales of ionization and recombination are long compared with HD timescales, especially for magneto-acoustic shocks. The shock temperatures are higher, and the intershock temperatures are lower, in models where time-dependent ionization is considered. This effect will likely change the range of parameter of the spicules type I (Leenaarts et al. 2007). Modeling the chromosphere is strongly important to study properly the radiative losses approximations, NLTE with scattering as has discussed by Carlsson (2010); Leenaarts (2010).

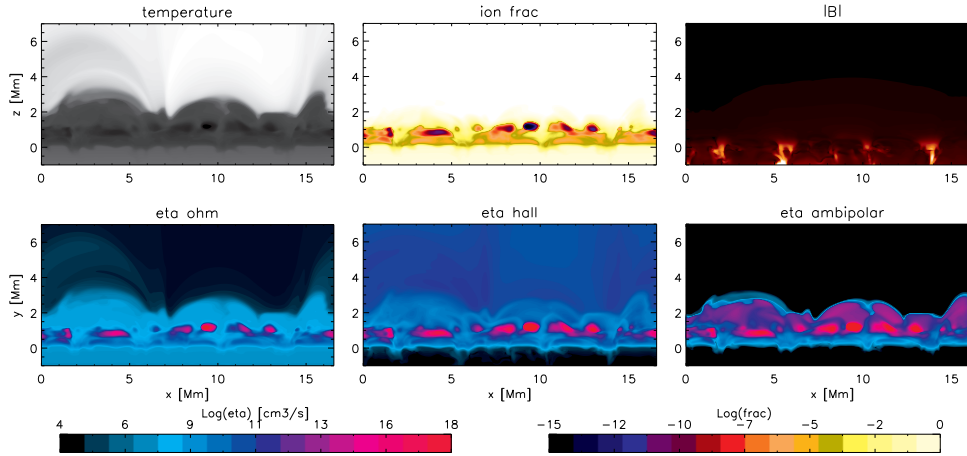


Figure 3. Temperature, ion fraction, magnetic field intensity, and ohm, hall and ambipolar diffusion calculated as post-processing in a 2D cut of the model, from left to right and top to bottom. Observe that Ohm and Hall diffusion are rather important in the lower chromosphere and the ambipolar diffusion in the upper chromosphere.

The partial ionization might have other effects on both types of spicules, as well. When considering partial ionization we find that ambipolar diffusion, Hall diffusion and ohmic diffusion contribute at differing rates throughout the chromosphere. The ratio between these three diffusion terms changes from the photosphere up to the transition region (see fig 3). This will possibly have important effects in the chromosphere as the parameters controlling reconnection and the damping of waves change.

Finally, we note that the range of ambient magnetic field structures that have been modeled only form a small subset of those expected when considering supergranulation, plage and the chromospheric network. In addition, a continuous weak magnetic flux emergence may need to be added, since it has been observed in the models that chromosphere and transition region heights are considerably increased with flux emergence.

Acknowledgments: Inestimable collaboration and contribution with Viggo Hansteen, Bart de Pontieu, Mats Carlsson and Fernando Moreno-Insertis.

References

- De Pontieu B. et al 2007, ApJ, 655, 624
 McIntosh S., et al., 2007, PASJ, 38, 219
 Rouppe van der Voort, et al., 2007, ApJ, 660,L169
 Hansteen V. H. et al. 2006, ApJ, 647, L73
 Leenaarts J., Carlsson M., Hansteen V., Rutten R. J., 2007, A&A, 473, 625
 De Pontieu, B. et al., 2009, ApJ, 701, L1
 Martínez-Sykora J., Hansteen V., Carlsson M., 2008, ApJ, 679, 871
 Martínez-Sykora J., Hansteen V., DePontieu B., Carlsson M., 2009, ApJ, 701, 1569
 Carlsson M., 2010, MmSAI, 80, 606
 Leenaarts J., 2010, in preparation